“Confinement effects for nano-electrocatalysts for oxygen reduction reaction”

Arezoo Avid[1] and Iryna V. Zenyuk[1*]

[1]Department of Chemical and Biomedical Engineering; National Fuel Cell Research Center, University of California, Irvine

221 Engineering Lab Facility, Building 323
University of California, Irvine
Irvine, CA 92697-3550
*e-mail: Iryna.zenyuk@uci.edu

Oxygen reduction reaction (ORR) is one of the most technologically relevant reactions. It occurs at the interface of the electrocatalyst and electrolyte, where oxygen reacts with protons and electrons to produce water. Because the electrocatalyst is dispersed on a high surface area support, morphological confinement becomes critical, as it dictates proton and oxygen transport. Furthermore, confinement is induced by ionomer, ionic liquids or molecular additives and their impact on electrocatalyst reactivity and transport properties is currently not well understood. We present an overview of electrostatics and mass transport induced confinement and zoom in into ionic liquids and molecular additives and try to unravel how local confinement induced by them impacts ORR.

Keywords: Nano confinement; electrocatalysts; oxygen reduction reaction; ionic liquids; electric double layers

1. Introduction

Oxygen reduction reaction (ORR) is critical for many technologies including polymer electrolyte fuel cells (PEFCs) and metal-air batteries. Platinum (Pt) or Pt-based alloys are used as electrocatalysts for ORR [1]. To maximize electroactive surface area of the Pt nanoparticles, they are dispersed on high surface-area supports, such as carbon blacks. **Figure 1** shows a schematic of carbon black particle, where Pt nanoparticles of 2-4 nm are on the surface and also within the micro-pores (< 2 nm) and meso-pores (< 50 nm). Perfluorosulfonated ionomer (PFSI) consisting of polytetrafluoroethylene (PTFE) backbone and sulfonic acid groups is added as a binder and proton conductor. Pt supported on carbon black and PFSI are casted onto a layer called catalyst layer. Recent study has shown that optimal catalyst support material should have the right amount of pores with size between 2 and 8 nm to avoid ionomer adsorption onto the catalyst, but at the same time effectively deliver oxygen to Pt within pores [2]. Due to size-exclusion, ionomer does not penetrate pores below 20 nm in size; therefore, in these pores, liquid water transports protons to the reaction sites [3]. Recent studies infiltrate ionic liquids (ILs) into carbon support pores and the resulting confinement effects help to promote ORR[4]. As oxygen, protons and electrons react in the ORR, they have a significant role in the confinement effects. The size of the micro- and meso-pores dictates the confinement for gas transport, as well as the proton transport due to electrostatics at solid-electrolyte interface. Confinement in thin-film ionomers is due to the polymer-catalyst interface, free surface interactions, and finite size effects [5]. Polymer properties, such as the backbone structure, equivalent weight, side-chain interaction with the substrate (specific adsorption etc.), and the chain entanglement impact the degree of confinement [6]. **Figure**

1 summarizes the confinement effects that are technologically relevant for ORR and will be overviewed in this work. Earlier review highlighted the recent experimental and modeling findings for single digit nanopores (< 10 nm), reviewing extreme confinement [7]. In addition, charge transport taking place in confined concentrated solution was reviewed in recent publication, as well, highlighting anomalous experimental results and break-down of classical theories [8].

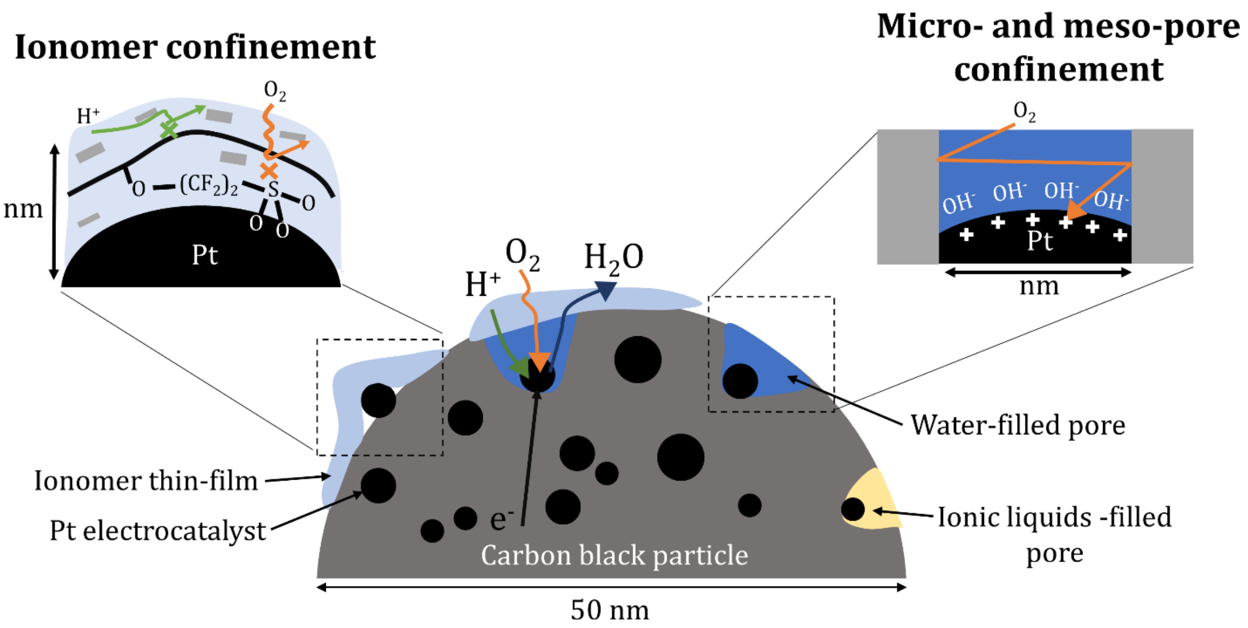

Figure 1. A schematic of a carbon-supported Pt electrocatalyst for ORR and associated transport phenomena. The interface between ionomer and Pt, and Pt within confined meso-pore are shown as well. Ionic liquids-filled pore is also shown in the schematic.

2. Nanoconfinement effects on ion transport

Electric double layers (EDLs) form at the interface between the electrocatalyst and electrolyte. They are present whenever two dissimilar phases are in contact and equilibrium is established after the contact. EDLs result in preferential water dipole orientation at the interface, separation of charge, electron spillover and may include specific adsorption. The outer Helmholtz plane (OHP) is the plane of the closest approach for solvated ions and the solution plane of the diffuse double layer. According to the classical Poisson-Boltzmann theory, EDLs diffuse layer thickness is expressed as the Debye length [9]:

$$\lambda = \sqrt{\frac{\epsilon RT}{F^2 \sum z_i^2 c_{i,bulk}}} \tag{1}$$

where, ϵ is the dielectric permittivity, R is the ideal gas constant, T is temperature, F is Faraday's constant, z is charge number and $c_{i,bulk}$ is bulk ionic concentration. Confinement effect is pronounced when the pore size is less than twice the width of the EDLs causing the double layers to overlap. **Figure 2a** shows the plot of the Debye length as a function of ionic strength of solution, where a linear profile on logarithmic plot is observed. Water at pH of 7 and Nafion are approximated to be 1 M solution. On the right y-axis, pore sizes corresponding to micro, meso- and macro-pores are shown. The shaded region represents scenarios, where pores will be filled with electrolyte of specific concentration considered to be under confinement. For example, the Debye length for Nafion is 0.3 nm; thus, there will be no confinement effect for ion transport in the pores with the size of 0.6 nm or larger. For ILs, the double layer thickness was measured to be several nanometers [10], whereas ionic strength is measured to be in a range between $(2.77 - 5.3) \times 10^3$ mol/m^3 [11]. When micro-pores are less than 5 nm and filled with ILs, overlapped EDLs will be present, resulting in confinement. **Figure 2b** shows the two potential distributions within the water-filled and Nafion-filled pore of 12 nm radius [12]. Due to the low ionic strength of water, the surface charge on Pt cannot be shielded by ions present in water; therefore, the potential lines are almost straight within the pore. On the other hand, the double-layer thickness for Nafion-filled pore is only 0.3 nm; therefore, most of the potential drop is within the metal-OHP region, and no confinement is observed. Since the driving force for Faradaic reactions is from metal to OHP, having thin double layers is beneficial for ORR.

EDL structure with IL molecules and polymerized ionic liquid[13] show drastically different behavior than EDLs of aqueous electrolytes, where complex ion ordering at the interface is an active area of research. This area includes the confinement effects[14] on EDL structure, potential[15][16] and molecular architecture dependency of the interfacial ionic layering[17][18]. Several works explore theories and models of the state of the ions in the ILs near the charged interface[19][20]. More applied studies focus on batteries performance with ILs[21], and tailoring the design of surface-active ILs to increase the energy density of the electrochemical device[22]. In their seminal work, Bazant et al.[23] proposed two modes for ion distribution near the charged metal surface: 1) at potential of 0.26 V, the surface is over-screened with a monolayer of counterions, whereas 2) at higher potentials (2.6 V) ion crowding extends to two monolayers. This model assumes monotonic charging of metal surface (**Figure 2c**). Our earlier work reviewed in-detail the role of proton transport on ORR for water-filled and aqueous electrolytes[24]. Marion et al.[25] measured ion conductivities of imidazolium type ionic liquids in nanopores of 20–600 nm size glass capillaries, observing no confinement effect down to 20 nm pores showing that ionic liquids behave as glass liquids.

Currently, ionomer confinement is generally studied with model systems[5], but is not well understood in actual catalyst layers. **Figure 2e** shows length-scales for ionomer confinement. Studies have shown that thin-film ionomers have reduced conductivity by 1/7th of that of the bulk[26],[27],[28], reduction in the water uptake [29], and through-plane water diffusion coefficient[30].

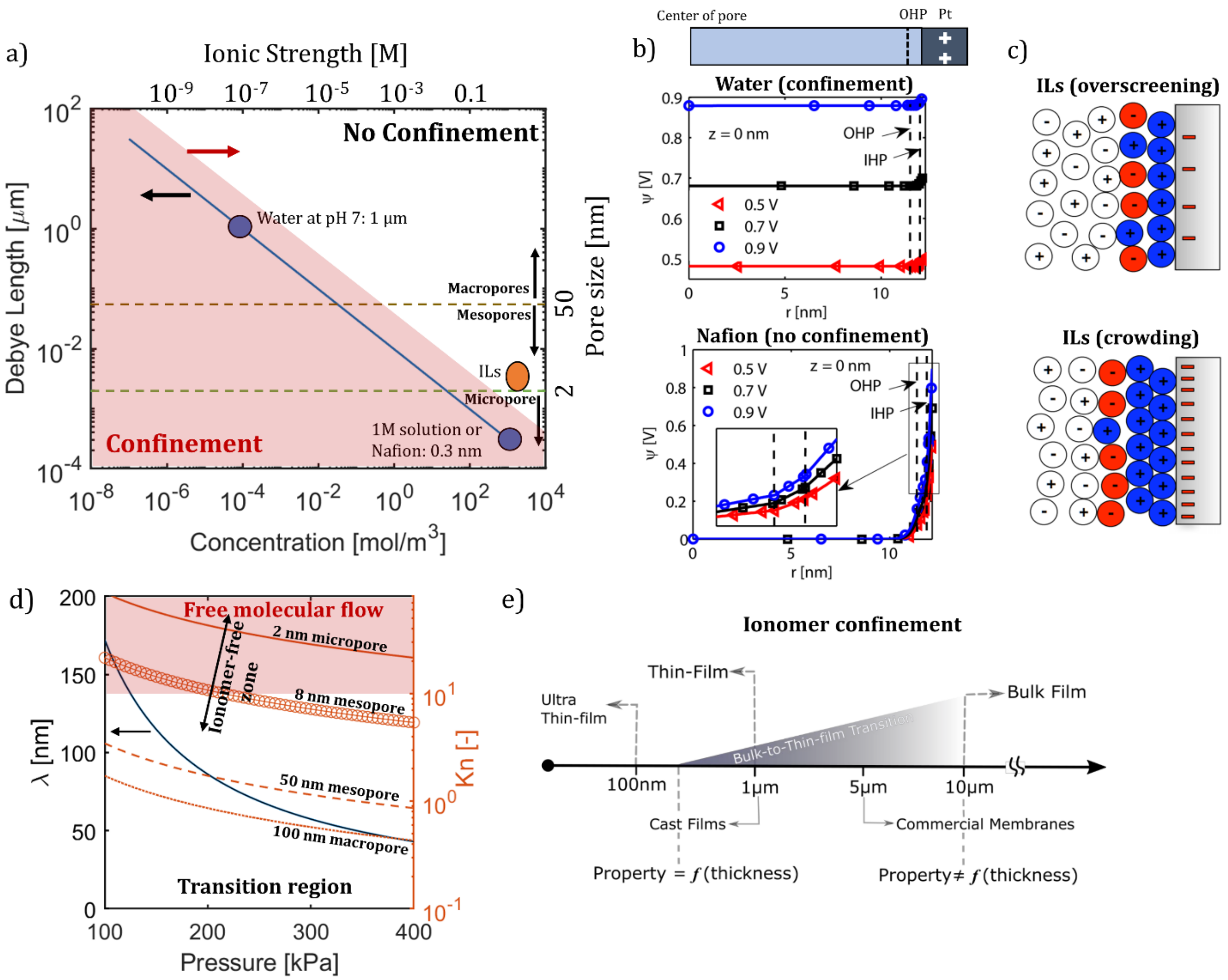

Figure 2. Confinement from the electrolyte perspective. a) Debye length as a function of ion concentration (or ionic strength), where linear relation is shown for aqueous electrolytes. Selected cases for DI water, 1 M solution or Nafion, and ILs are shown as well. The right-hand y-axis shown pore diameter and the shaded region represents definition of confinement. b) Potential distribution in 12 nm radius pore with Pt walls that is filled with water (top) and Nafion (bottom). Distribution for applied potentials of 0.5, 0.7 and 0.9 V are shown [12]. c) A schematic of ILs interface with a charged metal, where overscreening is observed for relatively low applied potentials (0.26 V), and ion crowding at interface is observed at high potentials (2.6 V) [23]. d) Gas mean free path for air as a function of gas pressure, where right y-axis shows Knudsen number. The Knudsen numbers for air in pores of 2, 8, 50 and 100 nm are shown too. Two regions of free molecular flow and transition regions are shown. e) Ionomer size from ultra-thin film to bulk film, where confinement effects are shown, adapted from [5].

3. Nanoconfinement effects on gas transport

Here we define gas confinement, when the molecule interaction with the wall is more frequent than the gas molecule-to-molecule collision. In meso- and micro-pores, there are two transport regimes characterized by two length-scales. The first one is the viscous regime in which thermal mean free path, $\lambda_T \ll L_C$, where L_C is the characteristic length-scale related to the dimension of the pore (for example a diameter for a cylindrical pore). The second transport regime is the free molecular flow, where $\lambda_T \gg L_C$, which was first investigated by Knudsen[31]. The Knudsen number, Kn is defined as a ratio of thermal mean free path to characteristic length-scale, $Kn = \lambda_T/L_C$. In viscous regime, defined as $Kn < 0.1$, no confinement exists, and continuum theory can be applied to study the gas transport. For $Kn > 10$, the free molecular flow, gas is confined by nanostructure of the pore and so-called Knudsen diffusion takes place. In the transition region $0.1 < Kn < 10$, pressure-driven flow coexists with diffusion transport[32]. As presented in the study by

Debe[33], the average time interval between oxygen molecules collision with the catalyst surface site determines the ORR rate determining step. In the Knudsen regime, the increased frequency of molecular collision with the pore wall will promote the ORR. **Figure 2d** shows mean free path for air across the range of pressure typically used in electrochemical conversion devices. Also, the Knudsen numbers are shown for the selected pores, where micro-pores and smaller meso-pores are located in the regime of the free molecular flow, as well as the pores where the ionomer is not present due to the size exclusion.

4. Ionic liquids and small molecules modifiers creating confined environment for ORR

For polymer electrolyte, which serves as a binder in the catalyst layer of the PEFCs, confinement can be described as a state where polymer chains are outside of their equilibrated state experiencing high strain. Both thin and ultra-thin films can generally be found in actual catalyst layers where the mechanical and transport properties of the ionomer thin film are modified due to the finite size effects[34]. Protons and oxygen gas are the reactants in the ORR. Although it was shown that protons do not participate in the rate-determining-step of the ORR[35], they can cause mass transport limitations when their transport is hindered by the confinements. In addition, oxygen gas transport is also affected by the confinements as described before; therefore, it is expected to observe an impact on the ORR activity induced by the confinement effects as will be discussed in the following studies.

One of the interface design principles for improving catalyst layer ORR performance is to infiltrate the micropores of the carbon support with a material that can fill the pores while facilitating sufficient proton and oxygen delivery to the Pt active sites (**Figure 1**). ILs are self-dissociative molten salts composed entirely of ions. Their unique characteristics such as high ionic conductivity, presence of protons in the cationic structure, negligible vapor pressure, thermal and electrochemical stability make them a promising additive to enhance the ORR in the cathode electrode of PEFCs [36][37]. They should also have low viscosity in order to be able to fill the pores without restricting O_2 diffusion. They should also possess high ΔpK_a value so that satisfactory proton transfer from the Bronsted acid to the base can be achieved due to the fast kinetics [38][39]. An IL with a higher O_2 solubility compared to aqueous media will increase the O_2 residence time within the pores filled with IL due to the confinement effect reported by Snyder et. al [40],[41]. As the O_2 molecule diffuses into pores, it is chemically biased to stay there, so the increased interaction frequency with the catalyst will decrease the ORR overpotential.

Finally, IL material should be hydrophobic as the increased O_2 solubility will facilitate the attraction of the reactants; therefore, the hydrophobic nature of ILs would help repulse the produced water out of the pores due to Le Chatelier's principle [40]. In addition, the hydrophobic microenvironment created by IL molecules prevents the Pt active sites from being oxidized and suppress the formation of oxygenated species. Therefore, the IL molecules protect the Pt active sites from being occupied by non-reactive species accelerating the ORR kinetics because strong Pt-O bonding is known to slow ORR [42].

The other interface design principle to enhance the ORR activity is to modify the catalyst with small molecules that can preserve Pt active sites by selective site-blocking mechanism (so-called third-body effect)[43],[44]. Wada et. al[45] reported that modification of single-crystalline Pt(111) surface with melamine molecule increases the activity by 3-fold compared to pristine Pt(111).

The effect of modifiers addition to Pt/C catalysts on cyclic voltammogram, polarization curve, and Nyquist plot is presented in **Figure 3**. Incorporation of ILs into Pt/C leads to a decrease in electrochemical surface area (ECSA) obtained from H_{UPD} peak (**Figure 3a**). This observation is known to be due to the selective site blocking effect of the IL and competition adsorption of IL ions with hydrogen atom [4],[40]. Moreover, strong ligand-type interactions of the IL molecule with Pt can weaken the Pt-H bonding [46]. The onset potential of Pt-oxide formation is shifted to a higher potential, and the area under OH_{ad} peak is decreased, indicating lower coverage of Pt active sites with oxygenated species. As shown in **Figure 3b**, the half-wave potential ($E_{1/2}$) is positively shifted to higher potential, indicating that catalyst activity is enhanced in the presence of the modifier. As summarized in **Figure 3c**, the linear portion of the Nyquist plot data at high frequencies is used for the calculation of the effective catalyst layer protonic resistance (R_{H^+}). The fitted line's intercept on the x-axis is considered to be $R_{H^+}/3$ [47]. As reported by Huang et al. [4] smaller protonic resistance is observed for Nafion-IL catalyst layer compared to the one with Nafion only, in addition to the fact that even excessive amount of IL will not restrict the diffusion of protons within the catalyst layer.

They explored a number of [MTBD]-based ILs with different anion structure, revealing the specific activity of the modified Pt/C catalyst has a linear relationship with the availability of Pt active sites ($1-\theta_{OH}$) and is not correlated with IL's oxygen solubility. Among all the ILs, [MTBD][$C_4F_9SO_3$] showed the highest ORR activity at the optimum IL/C ratio.

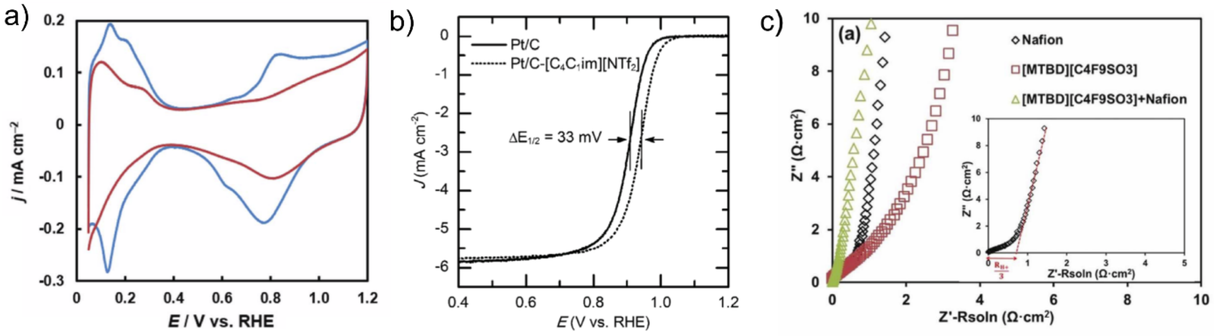

Figure 3. a) Cyclic voltammograms of Pt/C and Pt/C-[C_4C_1im][NTf_2] recorded in N_2-saturated 0.1 M $HClO_4$ solution, b) Polarization curves in O_2-saturated 0.1 M $HClO_4$ at 1600 rpm rotation rate from Zhang et al. [48], and Nyquist plots of impedance spectra under N_2-saturated 0.1 M $HClO_4$ for Pt/C-Nafion, Pt/C-IL and Pt/C-IL Nafion catalyst layers from Huang et al. [4].

Zhang et al.[49] studied the effect of pore-filling degree (α) and IL layer thickness on the ORR performance of 20 wt.% low surface area (LSA) carbon Pt/C-[MTBD][NTf_2] system by developing solid catalyst with ionic liquid layer (SCILL). They showed that at low pore filling degree, a part of Pt atoms is not fully in contact with O_2-enriched layer of the IL and the ORR kinetics cannot be sufficiently enhanced. On the other hand, a high α-value leads to an increase in the diffusion path to Pt surface, limiting the O_2 mass transport. Therefore, an optimal LSA Pt/C-[MTBD][NTf_2] system can be obtained with an α-value of 50%, boosting ORR activity sufficiently without high mass transfer resistance.

In another study, Zhang et al.[50] investigated the effect of alkyl chain lengths of imidazolium cations in 20 wt.% LSA Pt/C-[$C_nC_1$im][NTf_2] catalysts (n=2-10) on catalytic activity. It was disclosed that Pt/C-[C_4C_1im][NTf_2] has the maximum activity while showing ECSA value comparable to that of pristine Pt/C. ILs with long alkyl chains (n>6), form a lipid-/micelle-like rigid bilayer structure due to the aggregation of their nonpolar tail which leads to the repelling of the water molecules from Pt active sites protecting them from being oxidized; however, these IL molecules can block and interact with the terrace sites of Pt, decreasing the catalytic activity toward the ORR.

Asahi et al.[51] modified the commercial 46.1 wt.% high surface area (HSA) Pt/C catalyst with Melamine monomer without the presence of Nafion, and showed a mass activity enhancement factor of 1.8 and 30% decrease in the ECSA. They also reported the strong adsorption of low molecular weight poly(melamine-co-formaldehyde) methylated (PMF) on the Pt/C catalyst leads to an increase in the mass activity by 2-fold, although the ECSA is halved. **Figure 4** summarizes findings from electrochemical characterization of HSA and LSA Pt/C catalysts modified with various ILs, melamine small molecule, and low molecular weight PMF modifiers, and compares the optimum systems mentioned above.

Recent study by Yan et al. [52] reported a new approach in electrocatalyst design by replacing Nafion with poly(ionic liquid) as the proton conductor and binder. They synthesized block copolymers composed of an ionic segment facilitating the proton conduction and an aromatic ring-containing block (styrene) helping the oxygen transport to the electrocatalyst. They showed improved ORR performance with decrease in the fraction of the ionic segment to styrene block in the copolymer composition. Li et al.[53] optimized the local ionomer-electrocatalyst interface by developing a mixed ionomer system, Nafion/sulfonated poly(ionic liquid) block copolymer ionomer (SPILBCP). Nafion facilitates the bridging of SPILBCP isolated aggregates while establishing a connected ionomer network that helps the proton conductivity. As a result, catalyst layers developed with this method showed enhancement factor of ~2 in specific activity.

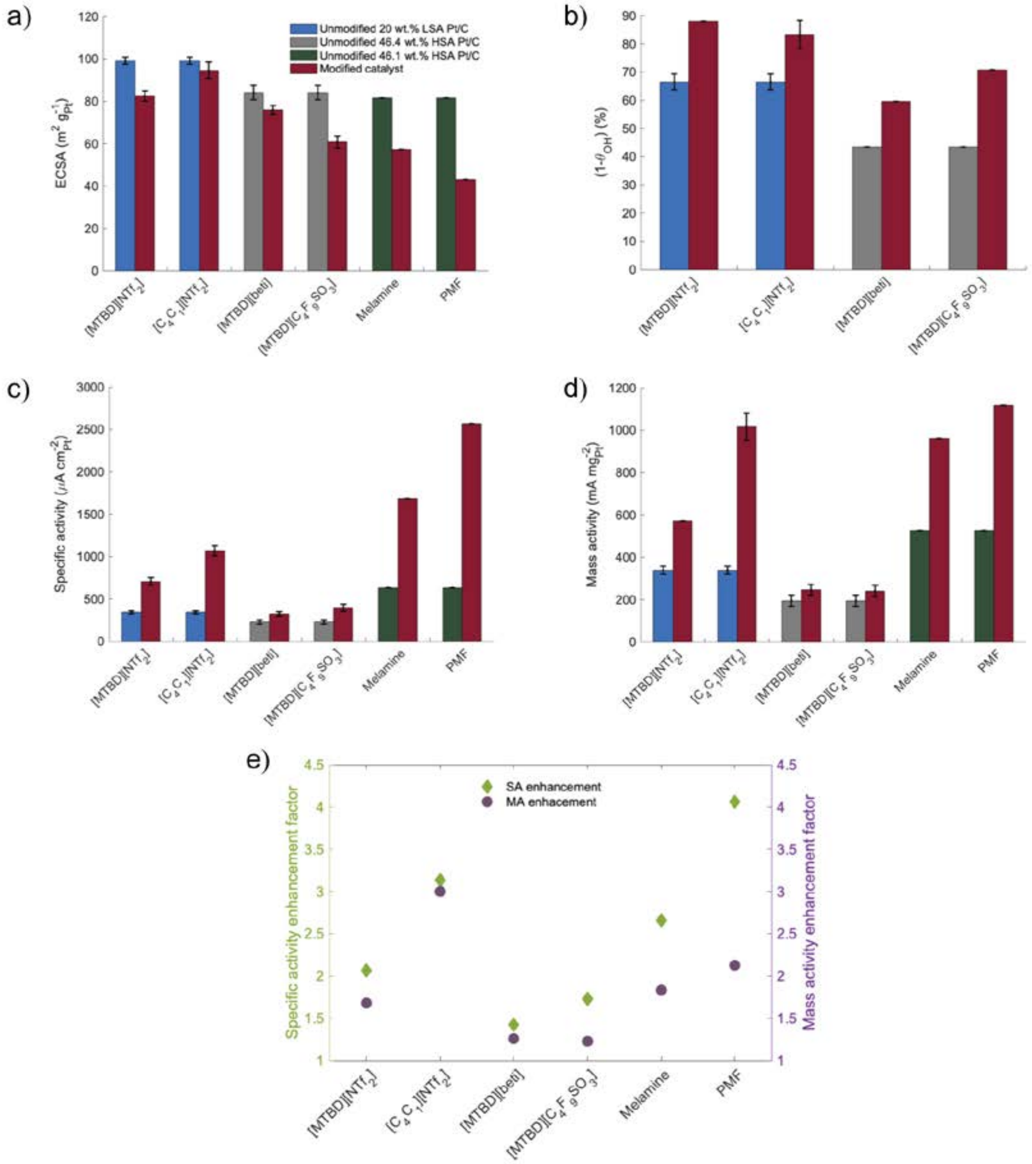

Figure 4. Comparison of electrochemical properties including a) ECSA, b) $1-\theta_{OH}$, c) specific and d) mass activity at 0.9 V on unmodified and modified LSA 20wt.% Pt/C catalyst with $[MTBD][NTf_2]$ from Zhang et al. [49], unmodified and modified LSA 20wt.% Pt/C catalyst with $[C_4C_1][NTf_2]$ from Zhang et al. [50], unmodified and modified HSA 46.4wt.% TKK catalyst with [MTBD][beti] and $[MTBD][C_4F_9SO_3]$ ILs adapted from Huang et al.[4], unmodified and modified HAS 46.1wt.% TKK catalyst with melamine molecule and low molecular weight PMF polymer modifiers[51]. e) Surface activity and mass activity enhancement factors for selected ionic liquids and two molecular modifiers.

5. Conclusions and Future Outlook

This review summarizes the recent studies on the nanoconfinement effects of the supported electrocatalysts and nanoconfinement due to infiltrated modifiers. Nanoconfinement is explored from the perspective of ORR, Knudsen diffusion of air molecules and ion transport in the nanopores based on the EDL thickness (Debye length), ionic strength of the material, and pore sizes. The implication for practical catalyst layers is the understanding of confinement and utilizing it to enhance the ORR which are critical for the interface design. For gas transport, Knudsen regime can be desirable as oxygen molecule is colliding with catalyst wall in this regime, which should enhance the ORR. By default, the micro- and smaller meso-pores within the catalyst layer will be filled with water (due to the ionomer size-exclusion). Utilizing modifiers can help: 1) increase the ionic strength of solution in small pores and reduce negative effects of EDLs overlap increasing the ion conductivity, 2) increase gas solubility values, 3) change the catalyst interaction with water (shifting oxide region) by inducing hydrophobic microenvironment. Interpretation of nanoconfinements and their role on ion conductivity and water molecules repulsion from Pt surface in the presence of different modifiers can help understanding the ORR kinetics dependence on the morphology of the carbon-supported electrocatalyst.

Acknowledgments

The author's work is supported by the National Science Foundation CAREER award 1652445.

References and recommended reading

*Paper of special interest
**Paper of outstanding interest

[1] X. Wang, Z. Li, Y. Qu, T. Yuan, W. Wang, Y. Wu, Y. Li, *Chem* **2019**, *5*, 1486–1511.

[2] N. Ramaswamy, W. Gu, J. M. Ziegelbauer, S. Kumaraguru, *J. Electrochem. Soc.* **2020**, *167*, 64515.

[3] I. V Zenyuk, S. Litster, *J. Phys. Chem. C* **2012**, *116*, 9862–9875.

[4] K. Huang, T. Song, O. Morales-Collazo, H. Jia, J. F. Brennecke, *J. Electrochem. Soc.* **2017**, *164*, F1448–F1459.
**Critical work on downselecting ILs for ORR activity and demonstrating that proton conductivity is reduced when ILs infiltrate the pores of the catalyst support.

[5] M. Tesfaye, Understanding the Impact of Confinement on Ionomer Thin Film Transport Properties, UC Berkeley, **2019**.
**A Ph.D. thesis documenting in-depth studies of confinement induced by thin film ionomer near metal catalyst interface.

[6] K. Kodama, K. Motobayashi, A. Shinohara, N. Hasegawa, K. Kudo, R. Jinnouchi, M. Osawa, Y. Morimoto, *ACS Catal.* **2018**, *8*, 694–700.
*Authors have shown specific adsorption and ionomer orientation for various single crystal Pt surfaces, showing how local ionomer confinement affects the ORR.

[7] S. Faucher, N. Aluru, M. Z. Bazant, D. Blankschtein, A. H. Brozena, J. Cumings, J. Pedro de Souza, M. Elimelech, R. Epsztein, J. T. Fourkas, et al., *J. Phys. Chem. C* **2019**, *123*, 21309–21326.
**An in-depth review of single digit pores and how confinement affects ion and gas transport, with application to braod set of technologies.

[8] Y. Gao, J. Huang, Y. Liu, S. Chen, *Curr. Opin. Electrochem.* **2019**, *13*, 107–111.
**Concise and relevant Current Opinion in Electrochemistry review, highlighting experimetnal anomalies critical to the ORR and other reactions explaining the need for advanced theoretical and computational tools to describe these.

[9] Z. Song, X. Cao, H. Huang, *Phys. Rev. E* **2018**, *98*, 32404.

[10] G. Krämer, F. Hausen, R. Bennewitz, *Faraday Discuss.* **2017**, *199*, 299–309.

[11] H. Tokuda, S. Tsuzuki, M. A. B. H. Susan, K. Hayamizu, M. Watanabe, *J. Phys. Chem. B* **2006**, *110*, 19593–19600.

[12] I. V Zenyuk, Interfaces in Polymer Electrolyte Fuel Cells, Carnegie Mellon University, **2013**.

[13] R. Kumar, J. P. Mahalik, K. S. Silmore, Z. Wojnarowska, A. Erwin, J. F. Ankner, A. P. Sokolov, B. G. Sumpter, V. Bocharova, *Sci. Adv.* **2020**, *6*, eaba7952.

[14] Y. D. Yang, G. J. Moon, J. M. Oh, I. S. Kang, *J. Phys. Chem. C* **2019**, *123*, 2516–2525.

[15] N. Nishi, J. Uchiyashiki, Y. Ikeda, S. Katakura, T. Oda, M. Hino, N. L. Yamada, *J. Phys. Chem. C* **2019**, *123*, 9223–9230.

[16] J. M. Klein, E. Panichi, B. Gurkan, *Phys. Chem. Chem. Phys.* **2019**, *21*, 3712–3720.

[17] S. Katakura, N. Nishi, K. Kobayashi, K. Amano, T. Sakka, *J. Phys. Chem. C* **2019**, *123*, 7246–7258.

[18] S. Watanabe, G. A. Pilkington, A. Oleshkevych, P. Pedraz, M. Radiom, R. Welbourn, S. Glavatskih, M. W. Rutland, *Phys. Chem. Chem. Phys.* **2020**, *22*, 8450–8460.

[19] Y. Avni, R. M. Adar, D. Andelman, *Phys. Rev. E* **2020**, *101*, 10601.

[20] G. Feng, M. Chen, S. Bi, Z. A. H. Goodwin, E. B. Postnikov, N. Brilliantov, M. Urbakh, A. A. Kornyshev, *Phys. Rev. X* **2019**, *9*, 21024.

[21] S. Begić, F. Chen, E. Jónsson, M. Forsyth, *Phys. Rev. Mater.* **2019**, *3*, 95801.

[22] X. Mao, P. Brown, C. Červinka, G. Hazell, H. Li, Y. Ren, D. Chen, R. Atkin, J. Eastoe, I. Grillo, et al., *Nat. Mater.* **2019**, *18*, 1350–1357.

[23] M. Z. Bazant, B. D. Storey, A. A. Kornyshev, *Phys. Rev. Lett.* **2011**, *106*, 46102.

[24] J. Liu, I. V Zenyuk, *Curr. Opin. Electrochem.* **2018**, *12*, 202–208.

[25] S. Marion, S. J. Davis, Z.-Q. Wu, A. Radenovic, *Nanoscale* **2020**, *12*, 8867–8874.

[26] D. Chen, A. Kongkanand, J. Jorne, *J. Electrochem. Soc.* **2019**, *166*, F24–F33.

[27] Y. Ono, Y. Nagao, *Langmuir* **2016**, *32*, 352–358.

[28] D. K. Paul, R. McCreery, K. Karan, *J. Electrochem. Soc.* **2014**, *161*, F1395–F1402.

[29] A. Kusoglu, T. J. Dursch, A. Z. Weber, *Adv. Funct. Mater.* **2016**, *26*, 4961–4975.

[30] S. A. Eastman, S. Kim, K. A. Page, B. W. Rowe, S. Kang, C. L. Soles, K. G. Yager, *Macromolecules* **2012**, *45*, 7920–7930.

[31] M. Knudsen, *Ann. Phys.* **1909**, *333*, 999–1016.

[32] G. Scorrano, G. Bruno, N. Di Trani, M. Ferrari, A. Pimpinelli, A. Grattoni, *ACS Appl. Mater. Interfaces* **2018**, *10*, 32233–32238.

[33] M. K. Debe, *J. Electrochem. Soc.* **2011**, *159*, B53–B66.

[34] A. Kusoglu, A. Z. Weber, *Chem. Rev.* **2017**, *117*, 987–1104.

[35] T. Y. George, T. Asset, A. Avid, P. Atanassov, I. V Zenyuk, *ChemPhysChem* **2020**, *21*, 469–475.

*A critical study by means of kinetic isotope effect, revealing that the ORR rate determining step on Pt/C and poly-Pt is proton independent.

[36] R. D. Rogers, K. R. Seddon, *Science (80-.).* **2003**, *302*, 792 LP – 793.

[37] T. Yasuda, M. Watanabe, *MRS Bull.* **2013**, *38*, 560–566.

[38] M. S. Miran, M. Hoque, T. Yasuda, S. Tsuzuki, K. Ueno, M. Watanabe, *Phys. Chem. Chem. Phys.* **2018**, *21*, 418—426.

*An overview of ionic liquids physiochemical properties including thermal stability, viscosity, and iconicity dependence on DpKa.

[39] A. J. Kresge, *Acc. Chem. Res.* **1975**, *8*, 354–360.

[40] J. Snyder, T. Fujita, M. W. Chen, J. Erlebacher, *Nat. Mater.* **2010**, *9*, 904–907.

[41] J. Snyder, K. Livi, J. Erlebacher, *Adv. Funct. Mater.* **2013**, *23*, 5494–5501.

[42] V. R. Stamenkovic, B. Fowler, B. S. Mun, G. Wang, P. N. Ross, C. A. Lucas, N. M. Marković, *Science (80-.).* **2007**, *315*, 493 LP – 497.

[43] D. Strmcnik, M. Escudero-Escribano, K. Kodama, V. R. Stamenkovic, A. Cuesta, N. M. Marković, *Nat. Chem.* **2010**, *2*, 880–885.

[44] Y.-H. Chung, S. J. Kim, D. Y. Chung, H. Y. Park, Y.-E. Sung, S. J. Yoo, J. H. Jang, *Chem. Commun.* **2015**, *51*, 2968–2971.

[45] N. Wada, M. Nakamura, N. Hoshi, *Electrocatalysis* **2020**, *11*, 275–281.

[46] M. Sobota, M. Happel, M. Amende, N. Paape, P. Wasserscheid, M. Laurin, J. Libuda, *Adv. Mater.* **2011**, *23*, 2617–2621.

[47] R. Makharia, M. F. Mathias, D. R. Baker, *J. Electrochem. Soc.* **2005**, *152*, A970.

[48] G.-R. Zhang, M. Munoz, B. J. M. Etzold, *Angew. Chemie Int. Ed.* **2016**, *55*, 2257–2261.

[49] G.-R. Zhang, M. Munoz, B. J. M. Etzold, *ACS Appl. Mater. Interfaces* **2015**, *7*, 3562–3570.

[50] G.-R. Zhang, T. Wolker, D. J. S. Sandbeck, M. Munoz, K. J. J. Mayrhofer, S. Cherevko, B. J. M. Etzold, *ACS Catal.* **2018**, *8*, 8244–8254.
*Authors showed improvement factor of 3 for both mass and specific activity when the alkyl chain length in the imidazolium cation is optimum in impregnated Pt/C catalyst.

[51] M. Asahi, S. Yamazaki, N. Taguchi, T. Ioroi, *J. Electrochem. Soc.* **2019**, *166*, F498–F505.
**This paper highlights the effect of PMF polymer compared to melamine small molecule in enhancing the ORR activity.

[52] X. Yan, F. Zhang, H. Zhang, H. Tang, M. Pan, P. Fang, *ACS Appl. Mater. Interfaces* **2019**, *11*, 6111–6117.

[53] Y. Li, T. Van Cleve, R. Sun, R. Gawas, G. Wang, M. Tang, Y. A. Elabd, J. Snyder, K. C. Neyerlin, *ACS Energy Lett.* **2020**, *5*, 1726–1731.
*The authors used ionic liquid modified Nafion (SPILBCP) to achieve enhancement of specific activity of 2 for ORR.